A Study of Harmonics in a Dedicated Cable Supply System to Feed EV Fast Chargers

Takuya Shoji and Taku Noda

***Abstract*--To achieve carbon neutrality by 2050, electric vehicles (EVs) are promoted and EV fast chargers are expected to become part of the public infrastructure. To feed power to EV fast chargers installed in highway rest areas, the authors have proposed a 33-kV dedicated cable supply system installed along the highway. Due to the large capacitance of a cable system, harmonics may be of concerns for the operation of the proposed system. Therefore, this paper presents a study of harmonics occurring in the 33-kV dedicated cable supply system to feed EV fast chargers. First, the cause of the harmonics is identified by deriving resonance frequencies of the equivalent circuit of the cable supply system. Then, the harmonic resonance phenomenon is verified by electromagnetic transient (EMT) simulations. The results indicate conditions with which harmonic resonance may occur in the cable supply system. To perform the simulations, the EMT simulation models of distribution substations and EV fast chargers are picked up from the generic EMT simulation models prepared in XTAP (eXpandable Transient Analysis Program) for distribution and microgrid simulations. It should be noted that the harmonics simulations mentioned above can readily be performed by picking up necessary models from the model library.**

***Keywords*: Distribution systems, Dynamic simulation, EMT simulation models, Electric vehicles (EVs), Fast chargers, and Harmonics.**

I. Introduction

CARBON neutrality by 2050 is now shared by the global community, and a large number of photovoltaic (PV) power generation systems and electric vehicles (EVs) are being interconnected to distribution systems [1], [2]. In particular, EV fast chargers are expected to become part of the public infrastructure. Currently, the number of EV fast chargers installed in publicly accessible locations is increasing, and the capacity of those chargers is also growing for achieving shorter charging time [3], [4].

To feed power to EV fast chargers installed in highway rest areas, the authors have proposed a 33-kV dedicated cable supply system installed along the highway [5]. Due to the large capacitance of a cable system compared with an overhead wire system, harmonics may be of concerns for the safe and stable operation of the proposed system. Therefore, this paper presents a study of harmonics occurring in the 33-kV dedicated cable supply system to feed EV fast chargers installed in highway rest areas. The possibility of harmonic interactions related to grid-connected inverters are reported in the literature [6]-[11]. Although harmonics due to EV fast chargers are also expected [12], [13], the number of reports is limited due to quite new installations. Therefore, the authors would like to add a simulation study utilizing electromagnetic transient (EMT) simulations. Traditionally, frequency-domain methods have been used for identifying harmonics occurring in power systems [14], [15]. Since EV fast chargers are new harmonic sources, the following strategy is taken in this paper. First, to understand the fundamental principles of the harmonics phenomenon, a simplified single-phase circuit of the cable supply system is used, and resonant frequencies are analytically derived by the system impedance seen from the EV fast charger in the frequency domain. In this way, the cause of the harmonics is identified for the fundamental case where EV fast chargers exist only in one rest area point in the system. Then, a detailed three-phase model of the cable supply system is built on the EMT simulation program XTAP (eXpandable Transient Analysis Program) [16], and EMT simulations are performed. The EMT simulations confirm the validity of the fundamental principles mentioned above. In addition, the EMT simulations are able to give results also for cases where EV fast chargers exist in more than one rest area point. The results indicate that harmonic resonance may occur when the length of the feeding cable is relatively short. This finding may be quite useful to install EV fast chargers in rest areas along a highway.

For the EMT simulations, the models of distribution substations and EV fast chargers are picked up from the generic EMT simulation models prepared in XTAP for distribution and microgrid simulations. It should be noted that the harmonics simulations mentioned above can readily be performed by picking up necessary models from the model library. Those generic EMT simulation models for distribution and microgrid simulations are introduced in Appendix A.

II. Harmonics in a 33-kV Dedicated Cable Supply System

A. 33-kV Dedicated Cable Supply System

Large-capacity fast chargers ranging from 150 kW to 350 kW are developed and deployed for realizing a shorter charging time, typically less than 30 minutes, which is similar

This work is supported by the following electric power companies in Japan: Hokkaido Electric Power Company, Tohoku Electric Power Company, Tokyo Electric Power Company Holdings, Hokuriku Electric Power Company, Chubu Electric Power Company, Kansai Electric Power Company, Chugoku Electric Power Company, Shikoku Electric Power Company, Kyushu Electric Power Company, and Okinawa Electric Power Company.

T. Shoji and T. Noda are with ENIC Division, Grid Innovation Research Laboratory, CRIEPI (Central Research Institute of Electric Power Industry), 2-6-1 Nagasaka, Yokosuka, Kanagawa 240-0196, Japan (e-mail: shoji3925@criepi.denken.or.jp; takunoda@ieee.org).

Paper submitted to the International Conference on Power Systems Transients (IPST2023) in Thessaloniki, Greece, June 12-15, 2023.

to those required for refueling gasoline engine cars [17], [18]. These fast chargers are planned to be installed in highway rest areas where a short charging time is desirable [19]. On a highway, EVs may often face a shortage of remaining battery level, and more than one fast charger will be installed in a highway rest area. The highway has rest areas not only in urban areas but also in countryside. Rest areas in countryside are often fed by a long distribution line with one or more voltage regulators. In this case, the impact of fast chargers on the power quality of the distribution line is concerned about.

As a solution to this problem, the authors have proposed a 33-kV dedicated cable supply system installed along a highway to feed EV fast chargers at multiple rest areas. A model case of this concept is shown in Fig. 1. In this model case, power is received at 33 kV from a substation close to one of the four rest area points to be fed, then a 33-kV cable line is installed along the highway to feed the rest areas. It is assumed that there are two rest areas, one for the up lanes and the other for the down lanes, at one rest area point. It should be noted that one rest area point includes two rest areas as mentioned above. Hereafter, make a clear distinction between a rest area point and a rest area. Altogether, eight rest areas exist at the four rest area points. The percent impedance of the transmission system to the receiving substation and the transformer used in the substation together assumed to be 0.082 p.u. on a 10-MVA basis. The distance between two neighboring rest area points is all 15 km, and the total length of the cable line is therefore 45 km. This system is dedicated only for feeding the EV fast chargers installed at the eight rest areas, and CVT 150 mm^2 is used for all sections. The specifications of the fast chargers are as follows. By assuming the same convenience as a gas station for refueling gasoline engine cars, six units of 350-kW EV fast chargers are installed in a rest area. For one rest area point, therefore, the total maximum demand is 4.2 MW. The EV fast chargers in the rest areas are fed by a low-voltage (LV) system whose voltage is 480 V, and this voltage is obtained by stepping down from the 33-kV supply or distribution system using a three-phase transformer. Fig. 2 shows a one-line diagram of a rest area point. Considering the all four rest area points, the total demand of this 33-kV distribution system is 16.8 MW.

To validate the model case, if the voltages and currents at all rest area points are within allowable ranges or not has been checked. The one-line diagram of the whole distribution system is shown in Fig. 3. The allowable voltage range is assumed to be from 31.5 kV to 34.5 kV, and the maximum current allowed is assumed to be 365 A. For this analysis, the power-flow tool called CALDG developed at CRIEPI has been used. Fig. 4 shows the voltage profiles for the full-load case (all EV fast chargers are working) and the no-load case (all EV fast chargers are not working) obtained by the power-flow calculation. From the full-load case, the voltage at the remote end where the largest voltage drop is observed is 31.9 kV which is within the allowable voltage range. In this full-load case, the maximum current is 306 A observed at the sending end. It is within the allowable current range as well. In the no-load case, however, the capacitance of the cables

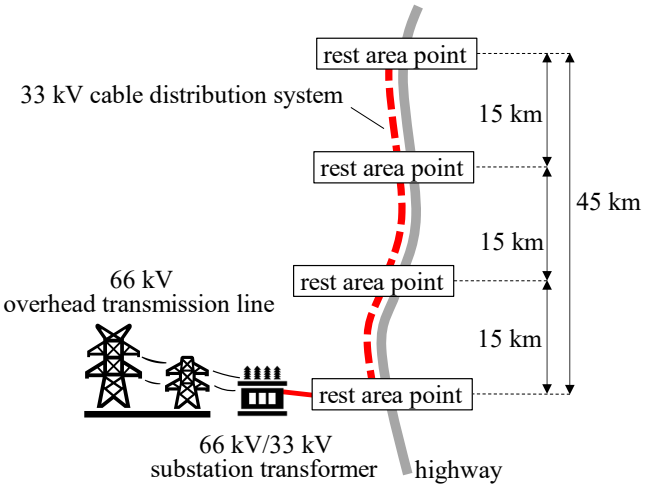

Fig. 1. Concept of the 33-kV dedicated cable supply system.

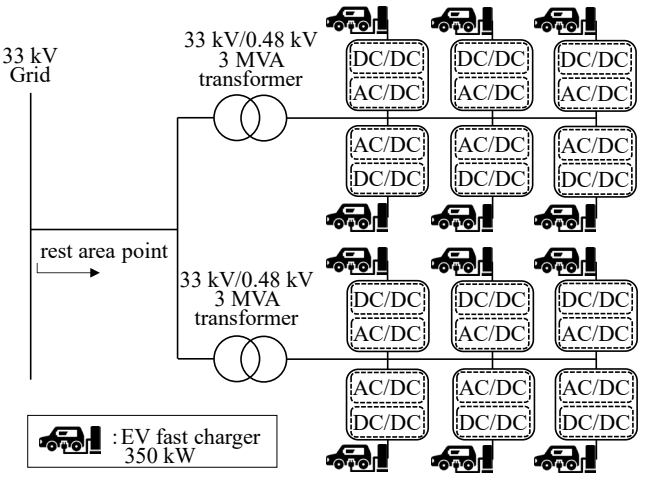

Fig. 2. One-line diagram of a rest area point.

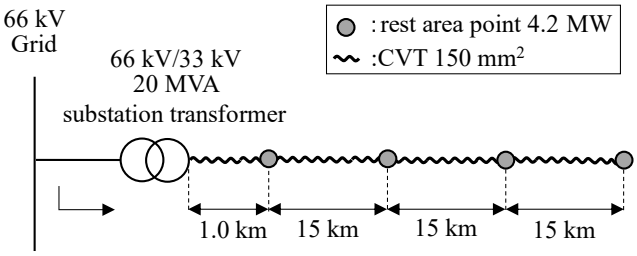

Fig. 3. One-line diagram of the whole distribution system.

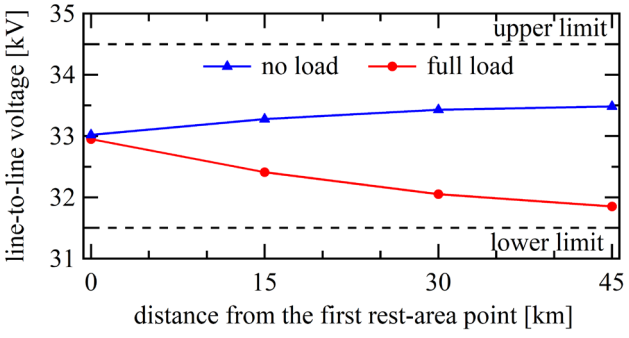

Fig. 4. Voltage simulation results for the full-load case (all fast chargers are on) and the no-load case (all fast chargers are off).

causes a Ferranti effect resulting in a voltage of 33.4 kV at the remote end. This is higher than the sending-out voltage but within the allowable voltage range. With this preparation, the validity of the model case has been confirmed.

B. fundamental Principles

An EV fast charger is basically an ac to dc power electronics converter. Generally, the harmonic filter of a power-electronics converter is designed so that it mostly eliminates harmonics generated by the conversion. Therefore, harmonics do not give a significant impact on the grid in most cases. As in the proposed cable supply system, however, a resonance phenomenon may occur, when a certain condition is satisfied due to the large capacitance of the cable system. The resonance may lead to a significant decrease in impedance at the resonance frequency. Large-capacity EV fast chargers are expected to have switching frequencies in the range from 2 to 9 kHz [12], [20], [21]. If the switching frequency of an EV fast charger coincides with the resonance frequency of the grid, then the resonance phenomenon leading to large harmonic voltages and currents may occur.

In this section, a simplified positive-sequence equivalent circuit is derived, and it is used for an analytical study of the phenomenon. Consider the simple case where a rest area point having 12 EV fast chargers which are fed by a dedicated cable. The upper part of Fig. 5 shows the equivalent circuit of the case in which the length of the cable is x m. Table 1 shows the parameters of the case. In Fig. 5, the 12 EV fast chargers are aggregated and represented by the voltage source E_h and the harmonic filter composed of L_f and C_f. The voltage source E_h approximates the harmonics by a sinusoidal wave whose frequency is equal to the switching frequency. Utilizing the superposition theorem, the voltage source that represents the system voltage at the power frequency can be short-circuited by focusing on the switching frequency of the ac to dc converter. Finally, the positive-sequence equivalent circuit shown at the lower part of Fig. 5 is obtained. If the grid side is seen from Point A, the admittance Y_g is expressed by

$$Y_g = j\,\frac{\omega^2 C_l L_u - 1}{\omega\{(L_u + L_{tr}) - \omega^2 C_l L_u L_{tr}\}} \tag{1}$$

The series resonance frequency is therefore given by

$$f_s = \frac{1}{2\pi\sqrt{\dfrac{L_u L_{tr}}{L_u + L_{tr}} C_l}} \tag{2}$$

and the parallel resonance frequency by

$$f_p = \frac{1}{2\pi\sqrt{L_u C_l}} \tag{3}$$

For instance, substituting x = 1 km into the equation above gives f_s = 2,558 Hz and f_p = 2,013 Hz. The frequency response is shown in Fig. 6 with the red curve. If the grid side admittance Y_h seen from Point B with x = 1 km is superimposed in Fig. 6, the blue curve is obtained. It has a series resonance frequency at 712 Hz and a parallel resonance frequency at 425 Hz, and the resonances at f_s and f_p can be observed on the blue curve but attenuated. To assess the impact in the grid, the frequency response of the voltage V_l at the cable with respect to the harmonic voltage source E_h is

TABLE I
SIMULATION PARAMETERS OF THE DEDICATED CABLE SUPPLY SYSTEM

	Parameter	Value (per unit)	1 rest area point
S_r	Rated power	350 kW	4.2 MW
V_{dc}	DC link voltage	1000 V	1000 V
V_{ac}	AC voltage	480 V	480 V
L_f	Inverter side inductor	495 mH (5 %)	41.3 mH
C_f	Filter capacitor	51.2 nF	1.84 μF
f_r	Filter resonance frequency	1000 Hz	1000 Hz
L_{tr}	Transformer used in the rest area point	92.4 mH (8.0 %)	46.2 mH
L_u	$L_u = L_s + L_t$ Upper voltage system inductor	28.4 mH	28.4 mH
L_s	Transmission system inductor	2.4 mH (0.7 %)	-
L_t	Transformer used in the substation inductor	26 mH (7.5 %)	-
L_l	Line cable inductor	629 μH/km	629 μH (1 km)
C_l	Line cable capacitor	0.22 μF/km	0.22 μF (1 km)

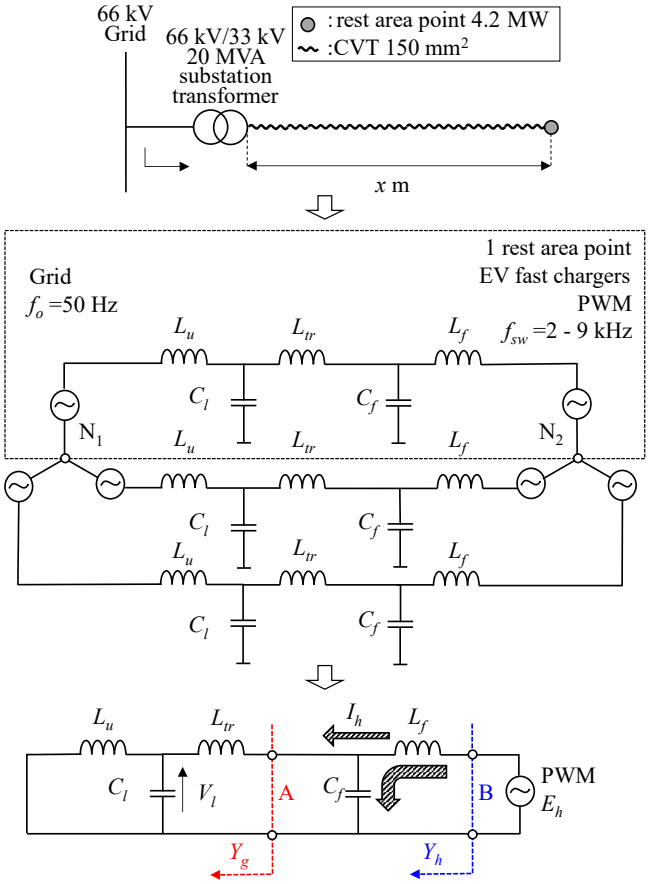

Fig. 5. A simplified positive-sequence equivalent circuit of a dedicated cable supply system.

calculated, and it is plotted in Fig. 7. It shows the two series resonance frequencies, one is from Y_h at 712 Hz and the other is from Y_g at 2,558 Hz. This frequency response suggests the following. When an 1-V voltage is applied at E_h, a high voltage occurs at the cable at 712 Hz and 2,558 Hz. Since the switching frequency of an EV fast charger is higher than 2

kHz, 712 Hz is not excited, but 2,558 Hz has a chance to be excited. As a result, most of the harmonics generated by the converter are eliminated by its harmonic filter, but some seep out into the grid. If the frequency of the harmonics coincides with the resonance frequency of the grid, then it is magnified at the cable.

To better understand this phenomenon, the voltage at the cable is calculated in the time domain, when an 1-V voltage is applied as E_h with different frequencies. The result is shown in Fig. 8 for 2,250, 2,550, 3,150, 4,050 and 4,950 Hz. As clearly observed from the result, when the frequency of E_h is 2,550 Hz which is the closest to the series resonance frequency of the grid, a magnified or resonant voltage is observed.

If the inductance L_u of the upper-voltage system and the inductance L_{tr} of the transformer are considered constant, then the series resonance frequency of the grid is dependent on the capacitance C_l or the length x of the cable. A shorter cable length gives a higher resonance frequency. If the switching frequency of the EV fast charger coincides with the resonance frequency of the grid, then it is magnified at the cable. This phenomenon should be noted when a feeding system for EV fast chargers is designed.

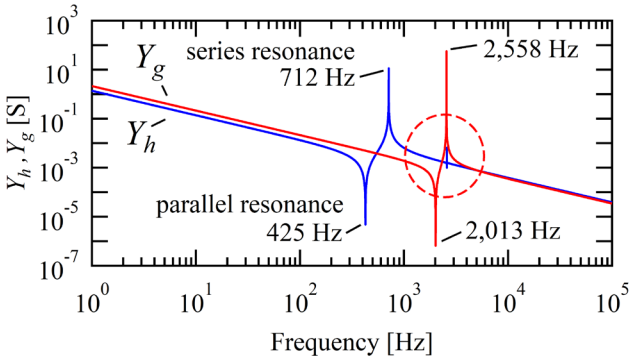

Fig. 6. Frequency responses of the admittance as seen from points A and B obtained by the simplified positive-sequence equivalent circuit.

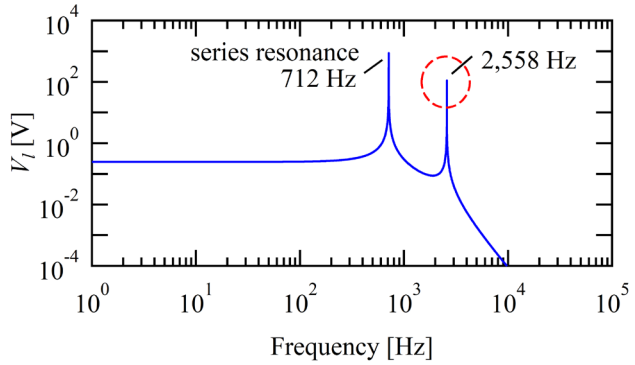

Fig. 7. Frequency response of the voltage at the cable obtained by the simplified positive-sequence equivalent circuit.

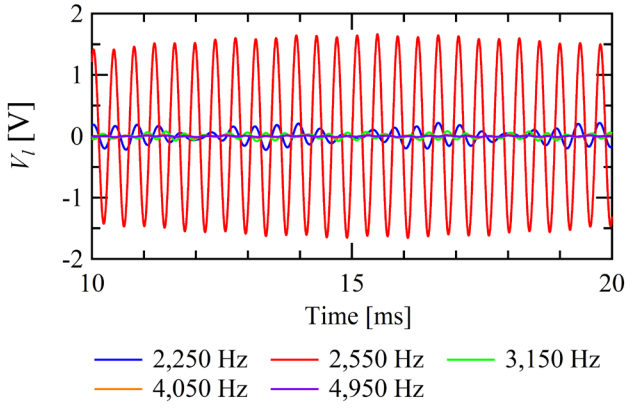

Fig. 8. Voltage at the cable in the time domain obtained by the simplified positive-sequence equivalent circuit for different frequencies.

C. EMT Simulations

As mentioned in Appendix A, XTAP is equipped with generic EMT simulation models for distribution and microgrid simulations. By picking up the distribution substation model and the EV fast charger model from the model library, EMT simulation cases have been created for the study performed in this subsection. The details of the distribution substation model and the EV fast charger model are shown in Fig. 9. Unlike the simplified equivalent circuit used in the previous

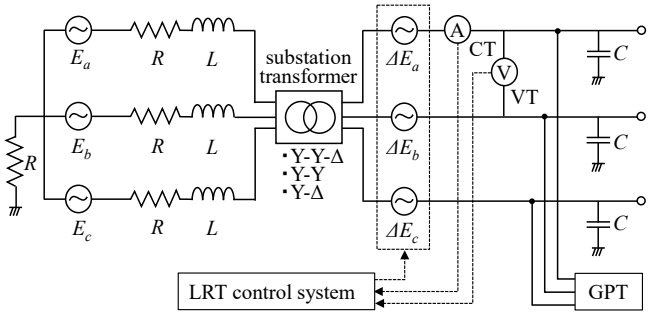

The three-phase voltage source E is used to generate the nominal voltage of the system, and the voltage source ΔE is added in series for the voltage adjustment corresponding to the change of the tap position of the LRT.

(a) distribution substation model

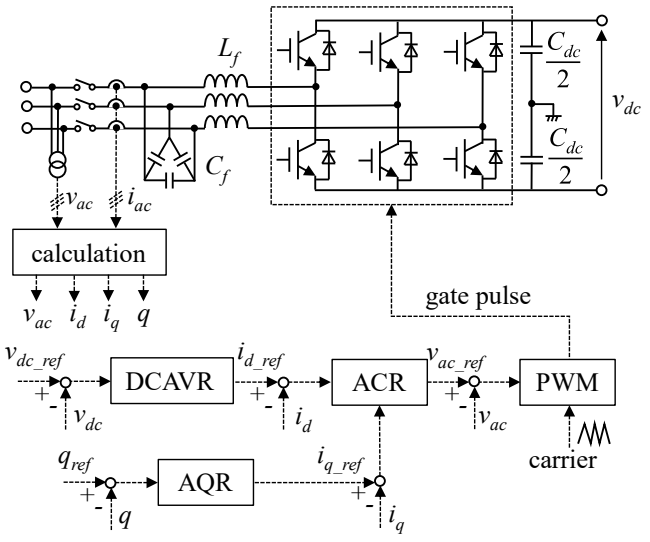

(b) EV fast charger model

Fig. 9. Details of the EMT simulation models used in the case study.

analytical study, all three phases including transformer winding connections and grounding resistances are represented in detail as shown in Fig. 10. The parameters shown in Table 1 are also used in this simulation. The EV fast chargers in one rest area point are aggregated to and represented by one equivalent EV fast charger model. The switching frequency of the EV fast charger is basically set to 2,550 Hz but varied in later cases.

Fig. 11 shows simulation results obtained by XTAP when the length of the feeding cable is varied as 1, 5, 10 and 15 km. The 33-kV three-phase cables are represented by a multiphase π equivalent circuit with coupling among phases. As shown in the previous analytical study, the resonance frequency of the grid becomes very close to the switching frequency when the cable length is 1 km. In this case, a resonance voltage is observed at the cable. Next, the switching frequency of the EV fast charger model is varied with the cable length fixed to 1 km. As seen in the simulation result shown in Fig. 12, a resonance voltage is observed at the cable when the switching frequency is 2,550 Hz among the other frequencies (see Appendix B for more detailed investigations). With the simulation results shown above, it is verified that the resonance phenomenon predicted in the previous analytical study also occurs in the detailed EMT simulations. It should be noted that the resonance voltages will not be observed in reality due to the operation of metal-oxide varistors. In reality, those metal-oxide varistors will be damaged by the resonance voltages.

Finally, the simulation model is extended to include four rest area points thus four cable spans. Fig. 13 shows frequency responses of the voltages at all four cables obtained by the frequency scan function of XTAP, when harmonic voltages are applied at the four rest area points with their phase angles aligned for simplicity. There are no resonance peaks in the range from 2 kHz to 10 kHz which is often used as the switching frequency of EV fast chargers. Fig. 14 shows the EMT simulation results. The resonance phenomenon does not occur for all different switching frequencies as observed by the frequency responses. It may be concluded that the presence of more than one rest area point suppresses the resonance phenomenon. As a result, the resonance phenomenon may occur when the resonance frequency of the grid coincides with the switching frequency of EV fast chargers in the case of one rest area point.

III. Conclusion

Due to the global trend, EVs are promoted, and EV fast chargers are expected to become part of the public

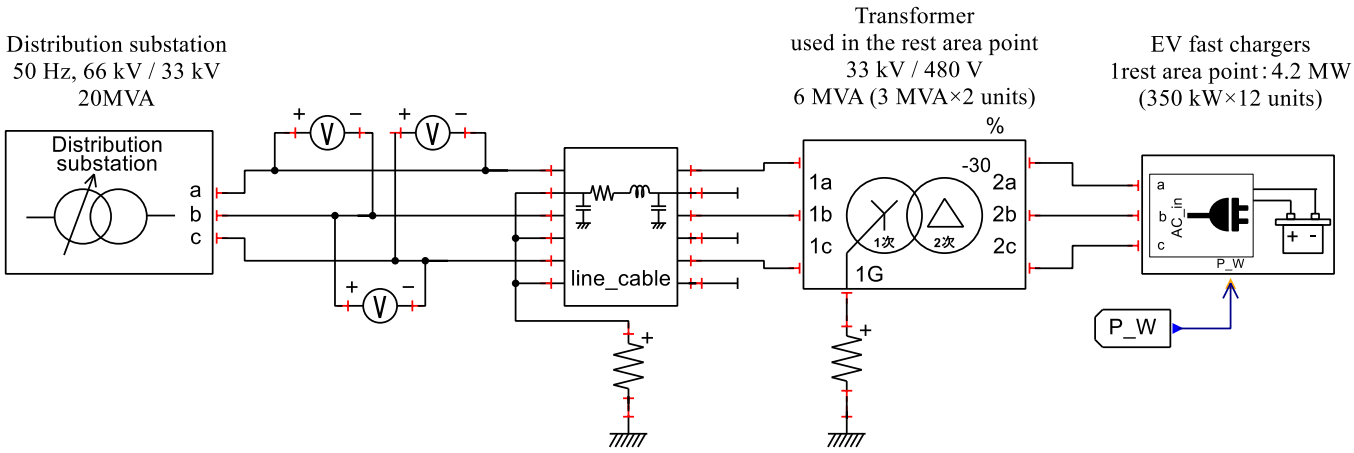

Fig. 10. Detailed three-phase EMT simulation model for feeding one rest area point.

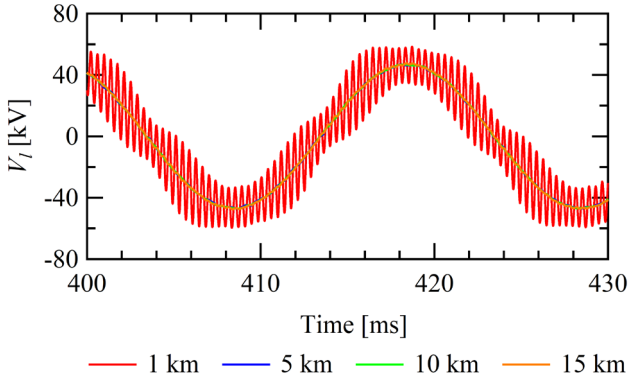

Fig. 11. EMT simulation results of the voltage at the cable for feeding one rest area point with fixed switching frequency at 2,550 Hz for different line lengths.

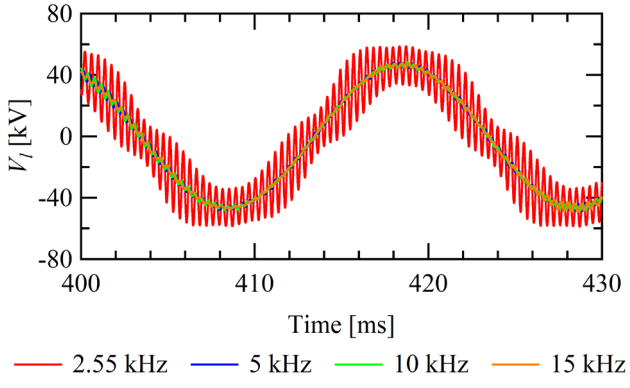

Fig. 12. EMT simulation results of the voltage at the cable for feeding one rest area point with the line lengths at 1 km for different switching frequencies.

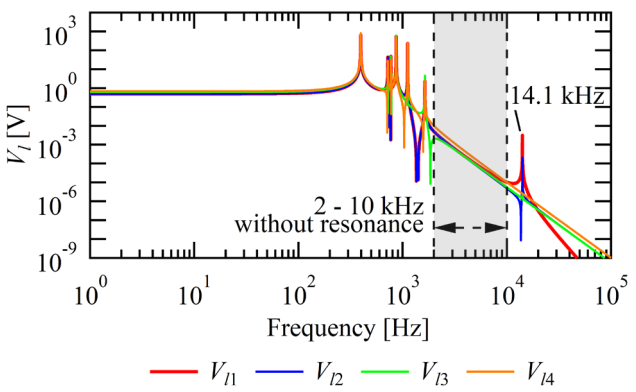

Fig. 13. Frequency responses of the voltage at all four cables on the load side when four rest area points are fed.

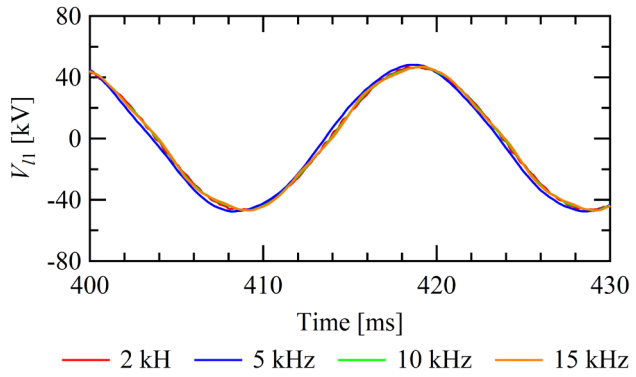

Fig. 14. EMT simulation results of the voltage V_{l1} at the cable when four rest area points are fed for different switching frequencies.

infrastructure. Prior to this publication, the authors have proposed a 33-kV dedicated cable supply system along a highway in order to feed power to EV fast chargers installed in highway rest areas. Due to the large capacitance of a cable system, harmonics may be of concern. In this paper, a study of harmonics occurring in the 33-kV dedicated cable supply system has been presented. First, the cause of the harmonics has been identified by deriving resonance frequencies of the cable supply system. Then, the harmonic resonance phenomenon is verified by detailed EMT simulations. As a result, it has been concluded that the resonance phenomenon may occur when the resonance frequency of the grid coincides with the switching frequency of EV fast chargers in the case of one rest area point. When the length of the feeding cable is about 1 km, the chances of resonance are high considering the switching frequency of EV fast chargers. This is a useful finding for those who design to install EV fast chargers in rest areas along a highway.

APPENDIX A
EMT SIMULATION MODELS FOR DISTRIBUTION SYSTEM STUDIES

Current distribution systems were mostly designed for unidirectional power flow from distribution substations to consumers, and their topology is radial. Recently-introduced PV power generation systems and EVs interconnected to distribution systems change the power flow which is now bidirectional and varying with respect to time. Under those situations, it is expected that the distribution system transforms into the platform to exchange electric energy among consumers and business entities. In order to realize such smarter distribution systems, interactions of control and protection algorithms among distribution and consumer devices must be avoided, and therefore simulation studies of the interactions play an important role [22]. In the past, studies of distribution systems required basic phasor-based simulations only. Dynamically-controlled components were the tap changer of the substation transformer and one or two step voltage regulators (SVRs) inserted in the middle of the distribution line to compensate the voltage drop of the load side. Modern studies of distribution systems, however, require EMT simulations in addition to the fundamental phasor-based simulations. Power-electronics converters used in PV power generation systems, EV chargers, and reactive-power compensators such as STATCOMs have fast control and protection systems, and thus EMT simulations are crucial. To facilitate such EMT simulations, the EMT simulation models of all possible distribution and consumer devices connected to distribution systems have been developed in XTAP, and their model icons are shown in Fig. 15, where the sub-figure alphabet letters correspond to the alphabet letters of the subsection headings below.

A. Distribution Substation Model

The distribution substation provides electrical power to a distribution system. The model represents the power source by a three-phase voltage source, the impedance seen from the distribution system, and the dynamics of the load-ratio transformer (LRT) for regulating the sending-out voltage.

B. Step Voltage Regulator Model

The step voltage regulator or the SVR is a three-phase autotransformer with a mechanical tap changer to compensate the voltage drop of the distribution line. The electrical circuit and the control system are represented in the model.

C. Thyristor Voltage Regulator Model

The thyristor voltage regulator or the TVR is a fast version of the SVR, and the mechanical tap changer is replaced by a thyristor circuit for fast and frequent operations. The electrical circuit and the control system are represented in the model.

D. PV Array Model

A number of PV modules connected in series and parallel are called a PV array. It is represented by an equivalent circuit with a nonlinear resistance whose *v-i* curve is determined by data shown in specification sheets provided by manufacturers.

E. Three-Phase Power Conditioner Model

The three-phase power conditioner (PCS) is used to convert dc power from a large capacity PV array to ac power so that it can be connected to the distribution system. It is

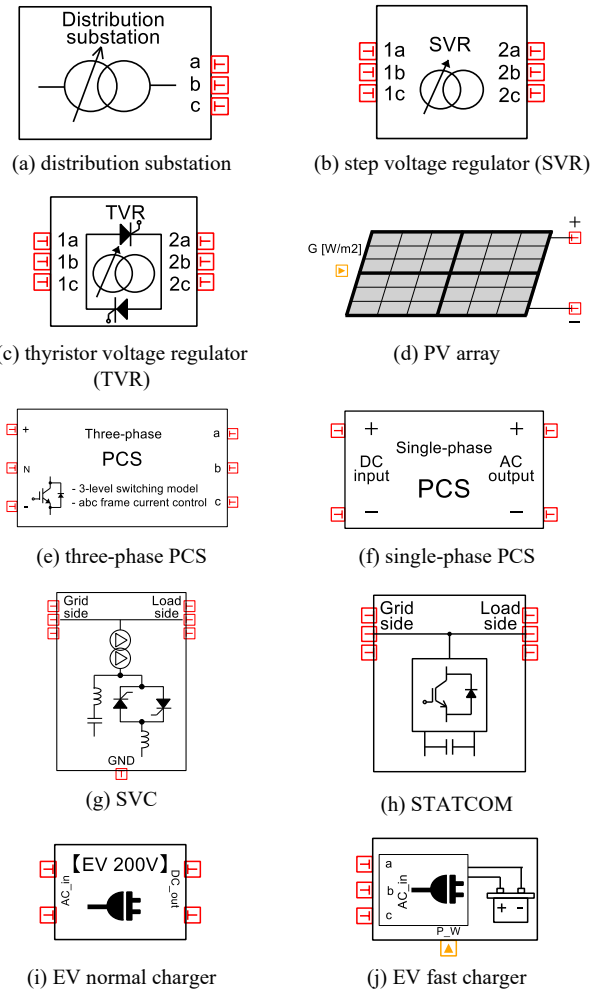

(a) distribution substation (b) step voltage regulator (SVR)

(c) thyristor voltage regulator (TVR) (d) PV array

(e) three-phase PCS (f) single-phase PCS

(g) SVC (h) STATCOM

(i) EV normal charger (j) EV fast charger

Fig. 15. Developed EMT simulation models of distribution and consumer devices.

basically a three-phase inverter with its control and protection systems including fault-ride-through (FRT) and islanding-detection relays. The power-electronics circuit and the control and protection systems are represented in detail in the model.

F. Single-Phase Power Conditioner Model

The single-phase power conditioner (PCS) is used to convert dc power from a small capacity PV array such as the one installed on a roof top to ac power for connection to the distribution system. It consists of a dc boost chopper and a single-phase inverter with their control and protection systems including an islanding-detection relay. The model represents the power-electronics circuit and the control and protection systems in detail.

G. SVC Model

The static var compensator or SVC is a reactive power compensator utilizing thyristors. It consists of a fixed capacitor bank which is also used as a harmonic filter, thyristor-controlled reactors (TCR) with a firing-angle control, and its control system. The model represents the power-electronics circuit and the control system.

H. STATCOM Model

The name stands for STATic synchronous COMpensator. The STATCOM is also a reactive power compensator, but it utilizes IGBTs (insulated-gate bipolar transistors) with a PWM (pulse width modulation) control. The power electronics circuit and its control system are represented in the model.

I. EV Normal Charger Model

The EV normal charger is used for normal (non-fast) charging of EVs. It uses the boost-type PFC (power factor correction) circuit to convert ac to dc for charging the battery of an EV. The model represents the PFC circuit and its control system in detail.

J. EV Fast Charger Model

This EV fast charger model is used in the harmonic simulations described in the main text of this paper. The details of the model are described in Section II-C.

APPENDIX B
IMPACT OF THE RATE OF RISE OF THE OUTPUT POWER

The charging characteristics of an EV fast charger can be represented by its rate of change of the output power. As a preliminary study of this point, the rate of rise of the output power is varied from 0.1 to 5.0 s in the EMT simulation case shown in Fig. 10 (Section II-C), and its impact on the harmonic waveform at the steady state is examined. The rate of rise of the output power from the EV fast charger is varied as 0.1, 1.0, 3.0 and 5.0 s as shown in Fig. 16. Then, it has been confirmed that the voltage waveform at the cable is in the steady state at t = 5.4 s for all cases. Those waveforms are plotted in Fig. 17. The four waveforms are almost identical, and it can be concluded that the impact of the rate of rise of the output power from an EV fast charger is negligible.

REFERENCES

[1] IEA (2021), Renewables 2021, IEA, Paris. https://www.iea.org/reports/renewables-2021

[2] IEA (2022), Global EV Data Explorer, IEA, Paris. https://www.iea.org/articles/global-ev-data-explorer

[3] IEA (2022), Global EV Outlook 2022, IEA, Paris. https://www.iea.org/reports/global-ev-outlook-2022

[4] Brown, Abby, Schayowitz, Alexis, & Klotz, Emily, "Electric Vehicle Charging Infrastructure Trends from the Alternative Fueling Station Locator: Third Quarter 2021," United States. https://doi.org/10.2172/1855378

[5] T. Shoji and T. Noda, "Power Quality Impact of EV Fast Chargers on Distribution Systems," Proc. of 2023 IEEJ Annual Meeting, vol. 6, no. 187, 2023.

[6] J. H. R. Enslin and P. J. M. Heskes, "Harmonic interaction between a large number of distributed power inverters and the distribution network," IEEE 34th Annual Conference on Power Electronics Specialist, 2003. PESC '03., 2003, pp. 1742-1747 vol.4, doi: 10.1109/PESC.2003.1217719.

[7] L. Hong, W. Shu, J. Wang and R. Mian, "Harmonic Resonance Investigation of a Multi-Inverter Grid-Connected System Using Resonance Modal Analysis," in IEEE Transactions on Power Delivery, vol. 34, no. 1, pp. 63-72, Feb. 2019, doi: 10.1109/TPWRD.2018.2877966.

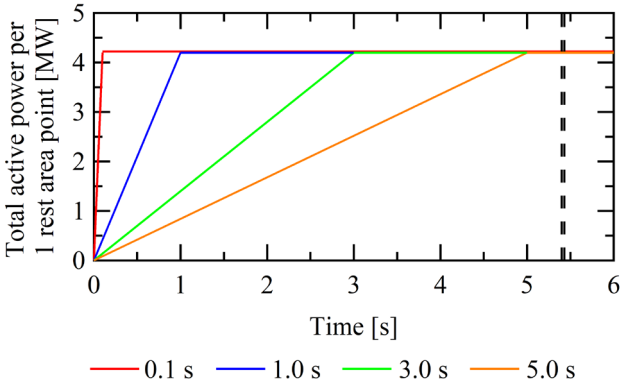

Fig. 16. Rate of rise of the output power from the EV fast charger used in the simulation study.

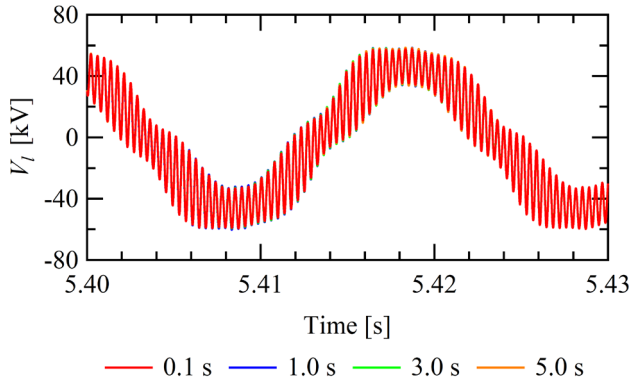

Fig. 17. EMT simulation results of the voltage at the cable for feeding one rest area point when the rate of rise of the output power from the EV fast charger is varied.

[8] S. S. Rangarajan, E. R. Collins and J. C. Fox, "Harmonic resonance repercussions of PV and associated distributed generators on distribution systems," 2017 North American Power Symposium (NAPS), 2017, pp. 1-6, doi: 10.1109/NAPS.2017.8107350.

[9] Z. Deng, M. D. Rotaru and J. K. Sykulski, "Harmonic Analysis of LV distribution networks with high PV penetration," 2017 International Conference on Modern Power Systems (MPS), 2017, pp. 1-6, doi: 10.1109/MPS.2017.7974392.

[10] J. L. Agorreta, M. Borrega, J. López and L. Marroyo, "Modeling and Control of *N* -Paralleled Grid-Connected Inverters With LCL Filter Coupled Due to Grid Impedance in PV Plants," in IEEE Transactions on Power Electronics, vol. 26, no. 3, pp. 770-785, March 2011, doi: 10.1109/TPEL.2010.2095429.

[11] H. Hu, Q. Shi, Z. He, J. He and S. Gao, "Potential Harmonic Resonance Impacts of PV Inverter Filters on Distribution Systems," in IEEE Transactions on Sustainable Energy, vol. 6, no. 1, pp. 151-161, Jan. 2015, doi: 10.1109/TSTE.2014.2352931.

[12] Y. Sun, E. C. W. de Jong, V. Cuk and J. F. G. Cobben, "Harmonic resonance risk of massive ultra fast charging station grid integration," 2018 18th International Conference on Harmonics and Quality of Power (ICHQP), 2018, pp. 1-6, doi: 10.1109/ICHQP.2018.8378897.

[13] Aiqiang Pan, Yongwei Zhu, Lijia Ren, Tiantian Chen, Sun Wen and Wang Yun, "Harmonic research of electric vehicle fast chargers," 2016 IEEE PES Asia-Pacific Power and Energy Engineering Conference (APPEEC), 2016, pp. 2545-2549, doi: 10.1109/APPEEC.2016.7779947.

[14] A. Bonner et al., "Modeling and simulation of the propagation of harmonics in electric power networks. I. Concepts, models, and simulation techniques," IEEE Trans. on Power Delivery, vol. 11, no. 1, pp. 452-465, Jan. 1996, doi: 10.1109/61.484130.

[15] A. Medina et al., "Harmonic Analysis in Frequency and Time Domain," IEEE Trans. on Power Delivery, vol. 28, no. 3, pp. 1813-1821, July 2013, doi: 10.1109/TPWRD.2013.2258688.

[16] XTAP web site. https://www.xtap.org/

[17] M. Safayatullah, M. T. Elrais, S. Ghosh, R. Rezaii and I. Batarseh, "A Comprehensive Review of Power Converter Topologies and Control Methods for Electric Vehicle Fast Charging Applications," in IEEE Access, vol. 10, pp. 40753-40793, 2022, doi: 10.1109/ACCESS.2022.3166935.

[18] N. Hussein and A. Massoud, "Electric Vehicle Fast Chargers: Futuristic Vision, Market Trends and Requirements," 2019 2nd International Conference on Smart Grid and Renewable Energy (SGRE), 2019, pp. 1-6, doi: 10.1109/SGRE46976.2019.9020974.

[19] "Government vision for the rapid chargepoint network in England," GOV.UK. https://www.gov.uk/government/publications/government-vision-for-the-rapid-chargepoint-network-in-england/government-vision-for-the-rapid-chargepoint-network-in-england

[20] X. Liang, S. Srdic, J. Won, E. Aponte, K. Booth and S. Lukic, "A 12.47 kV Medium Voltage Input 350 kW EV Fast Charger using 10 kV SiC MOSFET," 2019 IEEE Applied Power Electronics Conference and Exposition (APEC), 2019, pp. 581-587, doi: 10.1109/APEC.2019.8722239.

[21] D. Aggeler, F. Canales, H. Zelaya-De La Parra, A. Coccia, N. Butcher and O. Apeldoorn, "Ultra-fast DC-charge infrastructures for EV-mobility and future smart grids," 2010 IEEE PES Innovative Smart Grid Technologies Conference Europe (ISGT Europe), 2010, pp. 1-8, doi: 10.1109/ISGTEUROPE.2010.5638899.

[22] T. Noda, T. Kikuma, T. Nagashima and R. Yonezawa, "A Dynamic-Phasor Simulation Method with Sparse Tableau Formulation for Distribution System Analysis: A Preliminary Result," 2018 Power Systems Computation Conference (PSCC), 2018, pp. 1-7, doi: 10.23919/PSCC.2018.8442480.